https://doi.org/10.5194/cp-2022-63
Preprint. Discussion started: 22 August 2022

Climate of the Past
Discussions
Open Access

No changes in overall AMOC strength in interglacial PMIP4 timeslices

Zhiyi Jiang[1], Chris Brierley[1], David Thornalley[1], and Sophie Sax[1]

[1]Dept of Geography, University College London

Correspondence: Zhiyi Jiang (z.jiang.17@ucl.ac.uk)

Abstract. The Atlantic Meridional Overturning Circulation (AMOC) is a key mechanism of poleward heat transport and an important part of the global climate system. How it responded to past changes in forcing, such as experienced during Quaternary interglacials, is an intriguing and open question. Previous modelling studies suggest an enhanced AMOC in the mid-Holocene compared to the pre-industrial period. In earlier simulations from the Palaeoclimate Modelling Intercomparison Project (PMIP), this arose from feedbacks between sea ice and AMOC changes, which were dependent on resolution. Here we present an initial analysis of the recently available PMIP4 simulations. The ensemble mean of the PMIP4 models shows the strength of the AMOC does not markedly change between the *midHolocene* and *piControl* experiments or between the *lig127k* and *piControl* experiments. Therefore, it appears orbital forcing itself does not alter the overall AMOC. We further investigate the coherency of the forced response in AMOC across the two interglacials, along with the strength of the signal, using eight PMIP4 models which performed both interglacial experiments. Only 2 models show a stronger change with the stronger forcing, but those models disagree on the direction of the change. We propose that the strong signals in these 2 models are caused by a combination of forcing and the internal variability. After investigating the AMOC changes in the interglacials, we further explored the impact of AMOC on the climate system, especially on the changes in the simulated surface temperature and precipitation. After identifying the AMOC's fingerprint on the surface temperature and rainfall, we demonstrate that only a small percentage of the simulated surface climate changes can be attributed to the AMOC. Proxy records during the two interglacial periods paint a similar picture of minimal changes, which fits nicely with the simulated results. Although the overall AMOC strength shows minimal changes, future work is required to explore whether this occurs through compensating variations in the different components of AMOC (such as Iceland-Scotland overflow water). This lines of evidence caution against interpreting reconstructions of past interglacial climate as being driven by AMOC, outside of abrupt events.

1 Introduction

The Atlantic Meridional Overturning Circulation (AMOC) is a large system of ocean currents involving differences of the temperature and salinity between the water in the tropics and North Atlantic Ocean (Rahmstorf, 2006). It is made up of an upper cell which has two limbs, and a lower cell of northward flow of dense Antarctica Bottom Water (AABW, below 4000 m depth). The upper cell consists an upper limb of warm and salty northward surface flow (the North Atlantic warm current, up to 1200 m depth), and a lower limb of colder and deep southward flow (the North Atlantic Deep Water, 1500-4000 m depth)

https://doi.org/10.5194/cp-2022-63
Preprint. Discussion started: 22 August 2022

(Buckley and Marshall, 2016). The AMOC acts as a heat pump at the high latitudes as the meridional transportation brings warm water to the colder sub-polar and polar regions (Chen and Tung, 2018), then further modifies the climate in Northern Europe and the east coast of the North America (Găinuşă-Bogdan et al., 2020). It is responsible for producing about half of the global ocean's deep waters, sourced from the northern North Atlantic (Petit et al., 2021).

Since the AMOC plays a vital role in air-sea interactions, along with its ability to transport and redistribute heat and its effect as a carbon sink in the Northern Hemisphere (Gruber et al., 2002), studying the evolution of the AMOC strength in the past is of great importance for us. It helps us identify the mechanisms which lead to the AMOC changes (Buckley and Marshall, 2016), explain the recent global temperature changes (Tung and Zhou, 2013; Chen and Tung, 2014; Steinman et al., 2015), and make projections of the future climate. Comparison of the AMOC changes between different geological eras can provide us with a better understanding of the roles of the external forcing in the AMOC strength variations. In addition, past AMOC variations suggest that the distribution of surface heat and freshwater flux can affect the location of deep water formation and result in transient changes in the AMOC (Kuhlbrodt et al., 2007).

Our study focuses on investigating the AMOC changes during to interglacials, the *midHolocene* (6 ka Before Present) and *lig127k* (127 ka Before Present). These two simulations are palaeoclimate entry cards (Kageyama et al., 2018) for the Palaeoclimate Model Intercomparison Project (PMIP4) component of the current phase of the Coupled Model Intercomparison Project (CMIP6). The *lig127k* has been identified as a period of high interest (Tier 1 experiment) due to its higher average global temperature and sea level (Capron et al., 2017; Otto-Bliesner et al., 2017). It is considered a natural experiment for what climate may look like in the future and addresses one of CMIP's key questions: "How does the Earth system respond to forcing?" (Eyring et al., 2016). In the context of PMIP4, the focus lies on solar forcing due to the differences in Earth's orbit, while GHG concentrations and the continental configuration were similar (Otto-Bliesner et al., 2017). The *midHolocene* is another interglacial period with orbital forcing being the main difference, while other forcing remains very similar to the*piControl* experiment.

During the two interglacial periods, the orbital parameters are prescribed according to Berger and Loutre (1991). Eccentricity, the deviation of the Earth's orbit from a perfect circle, was larger (more elliptic) than that during the pre-industrial period, especially for the *lig127k*. Meanwhile, perihelion, the closest point in the orbit to the sun, occurred much closer to the boreal summer solstice in the *lig127k*. Obliquity, the tilt of the Earth's axis, was also higher during these two warm periods (Otto-Bliesner et al., 2017). This leads to a positive Northern Hemisphere summer insolation anomaly at both 127 ka and 6 ka, compared to pre-industrial, while the difference in total incoming insolation at the top of the atmosphere between the two periods is marginal (Otto-Bliesner et al., 2017). Due to the model differences in the internal model calendar and the impact of eccentricity and precession (the orientation of Earth's rotational axis) on the length of the seasons, the date of the vernal equinox must be fixed in all simulations to 21st March (Joussaume and Braconnot, 1997; Otto-Bliesner et al., 2017). More detail on the forcings and boundary conditions for the *lig127k* and *midHolocene* experiment can be found in Otto-Bliesner et al. (2017) and in Eyring et al. (2016) for the piControl experiment. Based on the experimental setup, the *midHolocene* and *lig127k*, when the seasonal insolation is the strongest forcing, are two reasonable periods to study whether or not the changes in orbital forcing have altered the overall AMOC strength in the two past interglacials compare to the *piControl* experiment.

https://doi.org/10.5194/cp-2022-63
Preprint. Discussion started: 22 August 2022

Climate of the Past
Discussions

After discussing the appropriate methods (Sect. 2), we first analyse the behaviour of AMOC during the Quaternary interglacials in individual PMIP4 models in Sect. 3, then we explore the AMOC variations during the past two interglacials based on the models ensemble mean, which are shown in Sect. 3.1. In Sect. 3.2, as the seasonal changes in incoming solar radiation amplified in the *lig127k* compared to the *midHolocene*, we investigated further to see whether the simulated response show similar amplification in these individual models or not. Meanwhile, we also devised a series of tests that must be passed for a forced response, and also try to identify the causes for the changes in AMOC that we see in individual models. Furthermore, since we have identified that the AMOC changes could leave a fingerprint on the surface temperature and precipitation variation in the *midHolocene*, as well as in the *piControl*, regressions of surface conditions against AMOC have been computed for each simulation runs for both *midHolocene* and *piControl*, and they are shown in Sect. 4.1. Based on the computed AMOC's fingerprint on the surface temperature and precipitation in individual models, we further estimated the percentage of simulated surface temperature and precipitation changes that can be explained by AMOC changes in Sect. 4.2, which is generally shown as the AMOC's role in global surface climate changes. After investigating the changes in AMOC and the role of AMOC in climate system in PMIP4 simulations, comparisons with proxy reconstructions for the Holocene and the last interglacial are discussed in Sect. 5.

2 Methods

Models used in this study are chosen based on their data availability. Twelve models in the Coupled Model Intercomparison Project phase 6 (CMIP6) provided 'msftmz' or 'msftmyz' as part of the Palaeoclimate Model Intercomparison Project phase 4 (PMIP4), with a single realisation per model. Meanwhile, 8 models performed both interglacial experiments. Details of the individual models are shown in Tab. 1. The data from FGOALS-f3-L used for the pre-industrial conditions comes from the *historical* simulation for years 1850 to 1899, as the AMOC variable is unavailable for the *piControl* simulation.

The AMOC intensity is computed using a modified version of Climate Variability Diagnostic Package (Phillips et al., 2014; Danabasoglu et al., 2012). Rather than using principal component analysis to define the AMOC (Danabasoglu et al., 2012), the maximum overturning streamfunction at 30°N is used (Zhao et al., 2022). Patterns of surface climate association with AMOC variations were computed via linear regression with the AMOC time series; precipitation regressions have been encoded to complement the existing surface temperature patterns (Zhao et al., 2022).

The maximum AMOC strength is defined as the maximum of the mean meridional mass overturning streamfunction below 500 m at 30°N (and additionally at 50°N), and the streamfuction is computed as zonal average. The simulated maximum AMOC strength at these two latitudes from individual models are used for the comparisons of the changes in the maximum AMOC between the interglacials and pre-industrial. The maximum AMOC usually occurs between 30°N to 40°N, yet the RAPID-MOCHA mooring array locates at 26°N, hence the 30°N is chosen. The choice of 50°N is due to the location of the OSNAP section (53-60°N). The data from the two arrays can provide us with estimations of the present-day AMOC strength for reference. If the latitudes of, say, 35°N or 55°N had been selected instead, the impacts on the results are subtle (Brierley et al., 2020) and would not effect the conclusions presented here.

https://doi.org/10.5194/cp-2022-63
Preprint. Discussion started: 22 August 2022

Table 1. Model simulation length (in years) and their AMOC at 30°N (in Sv, also with the standard deviation)

Model	Preindustrial		midHolocene		lig127k	
	Length	AMOC	Length	AMOC	Length	AMOC
CESM2	500	19.1±0.8	700	19.4±0.8	700	19.9±0.7
EC-Earth3-LR	201	15.0±2.1	203	16.2±2.7	210	18.6±1.4
FGOALS-f3-L	50	23.9±2.7	200	24.4±2.2	500	25.2±2.1
FGOALS-g3	699	32.8±2.5	500	33.5±1.9	500	33.4±2.1
GISS-E2-1-G	851	24.4±2	100	24.5±1.6	100	25.0±1.8
HadGEM3-GC31-LL	100	17.0±1.2	100	18.4±1.2	100	18.1±1.1
IPSL-CM6A-LR	1200	12.1±1.3	550	11.6±1.3	550	10.3±1.3
NorESM2-LM	391	21.2±0.9	100	21.4±0.8	100	21.6±0.8
INM-CM4-8	531	17.1±1.3	200	16.3±1.1	N/A	N/A
MPI-ESM1-2-LR	1000	20.1±1.2	500	20.1±1.4	N/A	N/A
MRI-ESM2-0	701	18.0±1.0	200	20.2±1.4	N/A	N/A
ACCESS-ESM1-5	900	19.5±1.1	N/A	N/A	200	22.5±1.6

All models are regridded on to a common 1° latitude grid with 61 levels of depth between 0-6000 m in the ocean to compute ensemble averages. All simulations are given equal weighting when the ensemble mean change in AMOC is computed.

A fingerprint of the AMOC on wider climate is computed separately for each simulation. The fingerprints are obtained by linearly regressing temperature / precipitation at each grid box over the globe onto AMOC maximum at 30°N, using the equation: $\delta T = \alpha \delta \Psi_{30N} + c$, where δ indicates an anomaly within a simulation, T is the temperature (at the grid point), Ψ the maximum overturning streamfunction at 30°N in the Atlantic, α is the fingerprint coefficient and c is a constant. A 15-month low-pass Lanczos filter is applied to the AMOC timeseries prior to computing the regression. Precipitation fingerprints are computed using percentage variations, rather than absolute rainfall anomalies. The percentage of local surface temperature changes that can be explained by AMOC changes, is then estimated by comparing simulated changes to the AMOC change multiplied by the regression coefficient (averaged between the interglacial and pre-industrial simulations) ($\Delta T_{\Psi}/\Delta T$). Similarly, the percentage of local precipitation changes that can be explained by the AMOC changes in each simulation can also be computed. However, in order to provide a less messy figure, the ensemble mean plot of the percentage of precipitation changes that can be explained by AMOC changes has been made instead. Firstly, we regridded all the models onto a common 1°× 1° grid, then take the average of each model's AMOC-induced precipitation changes (ΔP_{Ψ}), followed by taking the average of each model's simulated precipitation changes (ΔP). Eventually, the averaged ΔP_{Ψ} divided by the averaged ΔP provides us with the final results. Creating an ensemble mean plot by taking the average of each model's ratio ($\Delta P_{\Psi}/\Delta P$) leads to a chaotic image, because of division by minimal ΔP.

https://doi.org/10.5194/cp-2022-63
Preprint. Discussion started: 22 August 2022

3 Simulated AMOC during the *midHolocene* and *lig127k*

The first-order determinant on the AMOC strength is the model used for the simulation (Tab. 1). The AMOC strength at 30°N is highest in FGOALS-g3, with the rest of the models generally have results ranging from about 11.5-24.5 Sv. The highest simulated AMOC strength is more than twice of the lowest ones, even without FGOALS-g3. This feature was noted by Brierley et al. (2020) for the *midHolocene* simulations, who used the scatter-plot shown in the left panel of Fig. 1 to highlight this fact. The dashed green and pink vertical lines in Fig. 1 provide us with the information from direct observations in recent decades. The observational AMOC strength at 26°N which comes from the RAPID array (Rayner et al., 2011) is stronger than that at 53-60°N from the OSNAP section (Lozier et al., 2019; Srokosz et al., 2012). The AMOC strength from the simulation runs also reveals that the AMOC is stronger in the sub-tropical region than that in the sub-polar region (except for FGOALS-g3, Fig. 1). Furthermore, the largest difference of the maximum AMOC strength between 30°N and 50°N occurs in GISS-E2-1-G model in both the *midHolocene* and *lig127k* simulations, with a value of around 9.3 Sv. Significant difference is also shown in NorESM2-LM model, with a value of approximately 7.8 Sv in the 2 interglacial periods. Differences in other models generally are between 2 and 4 Sv. It should be noted that the observed AMOC strength at 53-60°N is computed in density coordinates (Lozier et al., 2019; Srokosz et al., 2012), whilst all the other values are computed in depth coordinates.

The interannual variability of the AMOC is also model-dependent (Tab. 1), and generally does not alter much between the various experiments. EC-Earth3-LR and the two models by FGOALS are the exceptions, but they do not provide coherent message about the response to increasing orbital forcing. Therefore, we consider these to be different samples from the same underlying distribution (Latif et al., 2022).

Brierley et al. (2020) adopted an arbitrary criteria to assess the importance of AMOC changes by shading the region where changes are less than 5% of the *piControl* AMOC strength. Only 4 out of 15 PMIP3 and PMIP4 models demonstrate a changes in *midHolocene* AMOC larger than this (Fig. 1 left panel). In addition, these 4 models all show a stronger AMOC in the *midHolocene* than that in the *piControl* experiment. The majority of the models do not demonstrate a substantial change in the maximum AMOC strength between this two periods either at 30°N or at 50°N (Tab. 1; Fig. 1 left panel). Brierley et al. (2020) state that these findings are consistent with the palaeo-reconstructions for the *midHolocene*, something discussed further in Sect. 5.

Similar results are seen when looking at the maximum AMOC strength in the *lig127k* and *piControl* in individual models (Fig. 1 right panel), the results are relatively similar to that in the *midHolocene*. There are 3 models (ACCESS-ESM1-5, EC-Earth3-LR and IPSL-CM6A-LR) that have a maximum AMOC strength exceeding 5% of the *piControl* strength at both 30 and 50°N. (The maximum AMOC strength in HadGEM3-GC31-LL at 30°N is slightly outside the 5% range as well, but AMOC at 50°N is not). The extent of these deviations are generally larger than those seen in the *midHolocene* (Fig. 1 left panel).

The distinct differences between model simulated results appear in the *lig127k* is well, with FGOALS-g3 still shows a very high simulated result of 33.4 Sv, and IPSL-CM6A-LR shows a low result of 10.3 Sv at 30°N. The large spread in the simulated maximum AMOC strength could be caused by models' discrepancies in the sensitivity to natural or anthropogenic forcing, or just model bias.

https://doi.org/10.5194/cp-2022-63
Preprint. Discussion started: 22 August 2022

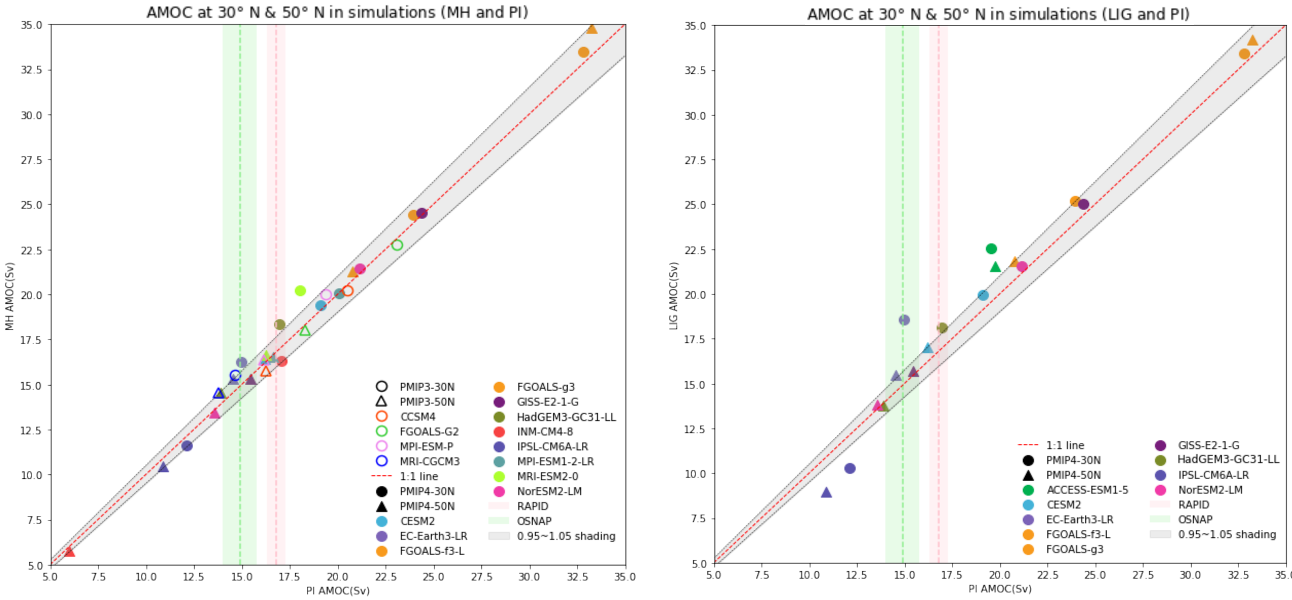

Figure 1. Maximum AMOC at 30°N and 50°N in preindustrial control simulations (horizontal axes) and interglacial simulations (vertical axes). Data points lying on the 1:1 line demonstrate no change between the two simulations. Observational estimates of the present-day AMOC strength are shown from both the RAPID-MOCHA array (26°N) and the OSNAP section (53–60°N). The mid-Holocene simulations from Brierley et al. (2020) are shown in the left panel; complemented by the last interglacial simulations shown in the right panel.

3.1 Ensemble mean AMOC changes

To explore the spatial patterns of changes in the AMOC structure in past warm interglacials, we compute PMIP4 ensemble mean AMOC changes (Fig. 2). The overlaid contours display the model averaged AMOC pattern in the *piControl* experiment to help place these changes in context. The two plots do not reveal a substantial change in the AMOC strength at the location where the maximum AMOC occurs (35-40°N,1000 m). There is a slight increase about 0.4-0.8 Sv in the maximum AMOC strength in the *midHolocene*, growing to 1.0-1.4 Sv in the *lig127k*. There is a slight intensification of the *midHolocene* model averaged AMOC strength at depth (up to 1.0-1.2 Sv at 2500 m in the sub-tropics). The *lig127k* experiments do not show such a focus of their intensification at depth, with the largest changes occurring in the top 500 m (Fig. 2b). An overall stronger AMOC in the *lig127k* is confined at the low-mid latitudes, as the AMOC strength becomes weaker in the sub-polar and polar regions (north of 55°N). Since the *midHolocene* and *lig127k* ensembles contain some different models, we additionally analyse the pattern of AMOC changes between the *midHolocene* and *lig127k* only using the models which have AMOC data in both of the periods (8 models in total). This demonstrates that the different increases in shallow (*lig127k*) and deep (*midHolocene*) branches are not an artefact of the additional models (Fig. 2c).

In all, although slightly larger changes in maximum AMOC are seen in *lig127k* than that in *midHolocene*, the maximum AMOC changes based on the ensemble mean during the past interglacials never exceed 1.5 Sv. This is definitely less than 10% of the respective *piControl* maximum strength, and generally less than 5%. There are some regions (such as at depth

https://doi.org/10.5194/cp-2022-63
Preprint. Discussion started: 22 August 2022

Climate of the Past
Discussions

in the *midHolocene*) that show greater proportional signals. However as with the AMOC strength, there are differences in the intensities of the AMOC pattern between individual models, but considering creating ensembles means of the percentage changes instead does not robustly alter our conclusions (not shown).

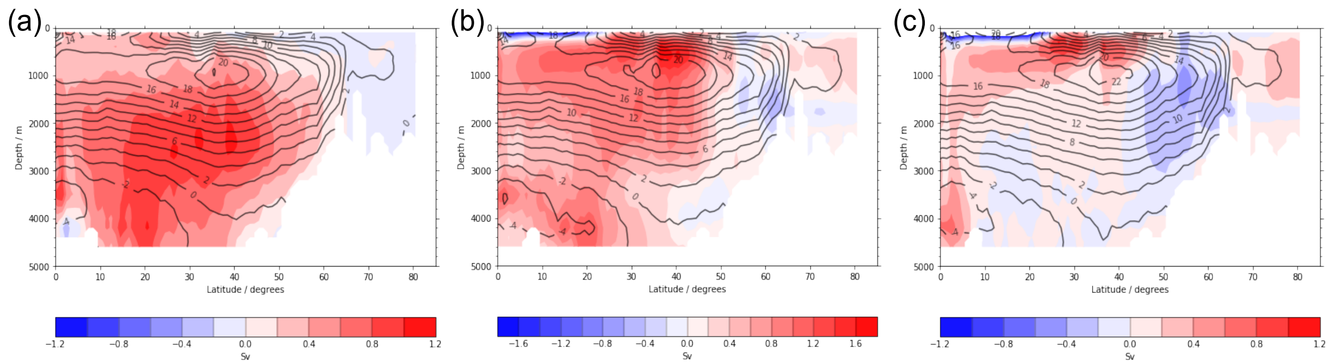

Figure 2. Ensemble, annual mean AMOC spatial structure changes in PMIP4. (a) Ensemble mean AMOC changes between the 11 PMIP4 models that have performed the *midHolocene* and *piControl* experiments. (b) Ensemble mean AMOC changes between the *lig127k* and *piControl* (consisting of 9 models). (c) Ensemble mean AMOC changes between the *lig127k* and *midHolocene* experiments (8 models). Overlaid black contours show model-averaged AMOC strength in the respective *piControl* simulations in (a) and (b), and in the respective *midHolocene* simulations in (c).

3.2 Assessing the forced response in AMOC

Since the seasonal changes in incoming solar radiation were amplified in *lig127k* compared to *midHolocene*, it would be expected (Williams et al., 2020) that the AMOC changes seen in the *lig127k* experiment are a similar, but stronger version of those seen in the *midHolocene* experiment. This is explored by analysing the AMOC profiles at 30°N for the 8 models which performed both interglacial experiments (Fig. 3). Only five models (CESM2, EC-Earth3-LR, FGOALS-f3-L, HadGEM3-GC31-LL and IPSL-CM6A-LR) show changes in AMOC in both experiments (at around 1000 m depth). The magnitude of amplification is very subtle in the CESM2 and FGOALS-f3-L models. The increases in AMOC shown between the *midHolocene* and *piControl* in the HadGEM3-GC31-LR model are actually slightly larger than those seen in the *lig127k* and attributed by Williams et al. (2020) as being a consequence of internal variability. The IPSL-CM6A-LR and EC-Earth3-LR model are the only 2, out of the 8 models, that demonstrate a noticeable, progressive changes from the *piControl* to *midHolocene* to *lig127k*. However, those 2 models show changes in opposite directions, with EC-Earth3-LR shows a positive response to the increased forcing, while the IPSL-CM6A-LR reveals a negative response.

To demonstrate that AMOC responds to orbital forcing, one would look for the ensemble to simulate AMOC changes that are (i) extant, (ii) related to the strength of the forcing, (iii) detectable over the internal variability and (iv) model independent. Building on these criteria, we devise a series of tests that must be passed to show a forced response within a single experiment. Firstly, we test whether there is a change in AMOC by judging whether the maximum AMOC strength at 30°N is not negligible, which here we arbitrarily take to be greater than 1 Sv. The changes in orbital configuration results in seasonal shifts in insolation

https://doi.org/10.5194/cp-2022-63
Preprint. Discussion started: 22 August 2022

Climate of the Past
Discussions

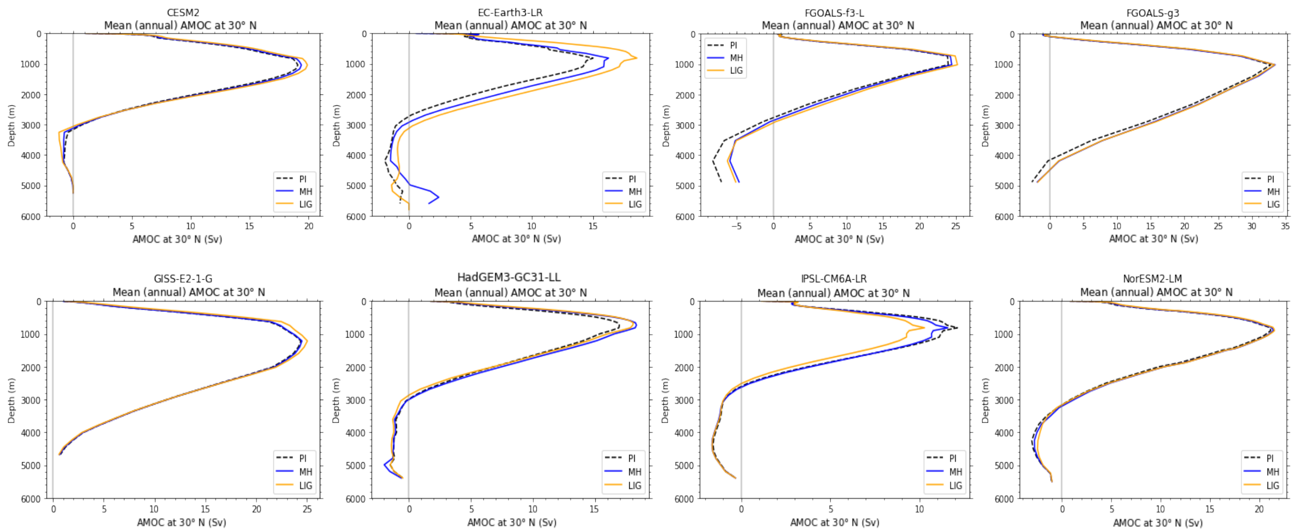

Figure 3. Mean (annual) AMOC profile at 30°N in simulations. The blue line shows the AMOC profile in the *midHolocene*, the amber line shows AMOC profile in the *lig127k*, and the dashed black line indicates *piControl* AMOC profile.

in the high Northern latitudes at in *lig127k* that generally more than twice as large than in *midHolocene* (Otto-Bliesner et al., 2017). The AMOC response may not be linear, so the second test sets a weaker threshold and looks at whether the AMOC changes in the *lig127k* are larger by half again than the *midHolocene* ones.

Assessing whether any AMOC changes are detectable against a model's internal variability in its AMOC timeseries is challenging given the relative lengths of the simulations (Tab. 1) and the known existence of low-frequency variability in AMOC (e.g. Fischer, 2011; Shi and Lohmann, 2016; McKay et al., 2018; Bonnet et al., 2021). The relative role of internal variability is assessed by comparing its strength to the size of the changes in the long-term mean. Whether an individual model has substantial low frequency internal variability are evaluated by firstly applying a 25-year low pass Lanczos filter to the annual mean AMOC timeseries of each simulation, then the Pearson correlation coefficients (r) are computed between the non-filtered timeseries and the filtered timeseries in each individual simulations. If the r^2 value is greater than 0.5, it suggests the low frequency variability dominates the AMOC timeseries (as it explains >50% of the AMOC variations). After inspection of the results for each individual simulation, we conclude that except for the IPSL-CM6A-LR and GISS-E2-1-G models, other models do not contain substantial low frequency variability according to this criteria. The IPSL-CM6A-LR is the only model for which all 3 experiments demonstrate substantial low frequency variability (Tab. 2). However, despite the CESM2 and EC-Earth3-LR models not meeting our particular criteria, the standard deviations of the filtered AMOC timeseries in these 2 models are at least half or more of the standard deviation of the non-filtered timeseries. Therefore, this suggests that low frequency variability plays an important role the CESM2 and EC-Earth3-LR models, even if it does not dominate the variability.

Only one of the eight models, EC-Earth3-LR, shows changes in AMOC that are categorised as both (i) extant and (ii) related to the strength of the forcing (Tab. 2). However, it is unclear if even these changes pass the 3rd criteria of detectability

https://doi.org/10.5194/cp-2022-63
Preprint. Discussion started: 22 August 2022

above internal variability - the amplitude of the *midHolocene* changes are less than one standard deviation of the interannual timeseries and there is also a confirmed presence of low frequency variability in the EC-Earth3-LR simulation (Zhang et al., 2021).

Clearly, the results of the individual tests performed here will depend somewhat on the criteria chosen. For example, if the maximum AMOC is taken anywhere North of 25°N then both CESM2 experiments would show extant AMOC changes, but only with the *lig127k* signal being only $1.3\times$ that of the *midHolocene* signal (Otto-Bliesner et al., 2020). However, two conclusions will remain robust to the many possible permutations. Overall the ensemble does not show a consistent AMOC signal from the imposed forcing changes. In fact, not a single one of the eight PMIP4 models that have performed both the *midHolocene* and *lig127k* experiments shows changes in AMOC strength that are unambiguously a response to the orbital forcing.

Table 2. Tests for assessing the forced response within a single simulation. The first 2 tests are based on the AMOC changes in the *midHolocene* and *lig127k* compared to *piControl*, where the change greater than 1 Sv is highlighted. The third test is based on the ratio of the AMOC changes in the *lig127k* to the AMOC changes in the *midHolocene*, and it is highlighted when the signal ratio is greater than 1.5. The last 2 tests involve the internal variability. The standard deviation of the unfiltered and 25-yr low-pass filtered AMOC timeseries are computed by averaging the standard deviation for each model in all 3 experiments, weighted by the respective run-lengths. The last row shows the number of experiments that have substantial low frequency variability ($r^2 > 0.5$) in each model based on the Pearson correlation coefficients (r) which show the relationship between the non-filtered timeseries and 25-yr low-pass filtered timeseries.

Tests	**CESM2**	**EC-Earth3-LR**	**FGOALS-f3-L**	**FGOALS-g3**	**GISS-E2-1-G**	**HadGEM3-GC31-LL**	**IPSL-CM6A-LR**	**NorESM2-LM**
Δ *midHolocene*	*0.3*	**1.3**	*0.5*	*0.7*	*0.1*	**1.4**	*-0.5*	*0.3*
Δ *lig127k*	*0.8*	**3.6**	**1.3**	*0.6*	*0.6*	**1.1**	**-1.8**	*0.4*
Signal Ratio	**2.7**	**2.8**	**2.6**	*0.9*	*6.2*	*0.8*	**3.4**	*1.4*
Std Dev.(unfiltered)	0.8	*2.1*	*2.2*	*2.2*	*1.9*	*1.2*	*1.3*	0.9
Std Dev. (low pass filtered)	0.4	*1.1*	*0.6*	*0.8*	*0.9*	*0.5*	*0.9*	0.4
Sims w. Low freq. variability?	0	0	0	0	1	0	3	0

4 AMOC and global surface climate changes

4.1 Unchanging AMOC fingerprints

We further investigate the role of AMOC in the interglacial climate system, particularly looking at the impact of AMOC on the simulated surface temperature and precipitation changes. First, we regress the temperature and precipitation at each grid

https://doi.org/10.5194/cp-2022-63
Preprint. Discussion started: 22 August 2022

Climate of the Past
Discussions

box over the globe onto AMOC maximum at 30°N for each simulation to obtain the local response to a 1 Sverdrup increase (see Sect. 2). Larger regression coefficients indicate that the interdecadal variability in the AMOC has more impact on the surface temperature or precipitation changes at each grid box. There is a strong relationship between AMOC change and surface temperatures over the northern North Atlantic, and they are most obvious in the Nordic Seas, south of Greenland, Labrador Sea and along the track of the Gulf stream (Fig. 4). This reveals that the AMOC has a noticeable influence on modulating the surface temperature through heat transport in those regions (Borchert et al., 2018; Jungclaus et al., 2014). The regression coefficients are generally higher in the Nordic Seas than that in the area in south of Greenland when referring to all the 11 PMIP4 models involved (not shown). The area of influence is generally confined to the northern North Atlantic (Fig. 4), although the FGOALS-g3-L and GISS-E2-1-G models both have particularly low coefficient values (~ 0.15) even there (not shown). Here we present regression coefficients from the *midHolocene* simulations, yet these are effectively unchanged in either the *piControl* or *lig127k* simulations (not shown).

The AMOC temperature fingerprints in the North Atlantic are accompanied by a dipole response in precipitation (Fig. 4) with roughly a 5% decrease in the mid-latitude (30-50°N) and a 5% increase in the subpolar and polar regions. The largest AMOC-induced precipitation changes occur in the Tropics - with a reduction of about 10-15% in the Equatorial Pacific. The FGOALS-f3-L (not shown) and NorESM2-LM show a larger decrease than other models (20-30% and 30-40%, respectively). Low latitude (0-30°N) North Atlantic ocean generally reveals an increases (up to 10%) in rainfall as the AMOC changed by 1 Sv, and it is more obvious in IPSL-CM6A-LR and NorESM2-LM. The 25% / Sv change in the increasing of precipitation in NorESM2-LM, which can be explained by the northward shifting of the Intertropical Convergence Zone (ITCZ) due to the stronger AMOC at this region, and it further results in more precipitation. NorESM2-LM shows the largest changes across the whole globe (Fig. 4) and is somewhat of an outlier. The fingerprints are very similar if computed using either *piControl* or *lig127k* simulations (not shown) - demonstrating that influence of AMOC is robust feature in the models with minimal state dependence. It should be noted that despite these fingerprints being computed from analysis of the internal variability within individual simulations, the spatial patterns are clearly reminiscent of those seen in hosing experiments (e.g. Jackson and Wood, 2020), demonstrating their appropriateness for the analysis performed here.

4.2 The role of AMOC in global surface climate changes between *midHolocene*, *lig127k* and PI

Having identified the AMOC fingerprints and additionally computed the AMOC changes in the experiments, we can estimate the percentage of the simulated *midHolocene* surface temperature change that can be explained by the AMOC changes (Fig. 5). Naturally, this percentage can approach, or even exceed, 100% when the simulated *midHolocene* changes are very small. In addition, areas with percentage smaller than 0 can occur when the AMOC fingerprint suggests changes of the opposite sense as the actual changes. Both cases indicate that the AMOC changes can not explain the *midHolocene* temperature response in those areas.

The four models with the largest changes in maximum AMOC strength at 30°N (see Fig. 1) show that around 40% of the simulated mid-latitude NOrth Atlantic surface temperature change can be explained by AMOC changes (Fig. 5. IPSL-CM6A-LR and MRI-ESM2-0 show a higher percentage (40-60%) in the North Atlantic ocean, as well as a very large percentage

https://doi.org/10.5194/cp-2022-63
Preprint. Discussion started: 22 August 2022

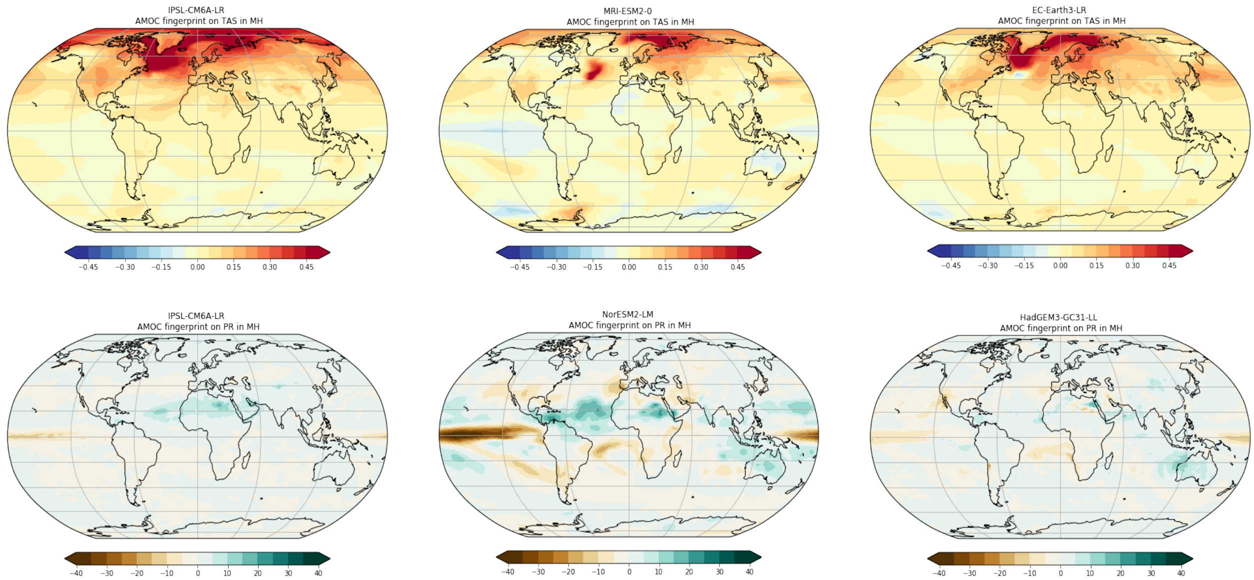

Figure 4. AMOC's fingerprint on the surface temperature (upper panels, unit: °C / Sv), and on the precipitation (lower panels, unit: % / Sv) in the *midHolocene* in selected PMIP4 models.

(60-80%) of surface temperature changes in the Nordic Seas coming from their AMOC changes. In the EC-Earth3-LR and HadGEM3-GC31-LL models, there are areas where around 30-40% of the simulated surface temperature change can be explained by AMOC changes. Slightly higher percentage can be seen in very confined areas. The 2 models, along with the IPSL-CM6A-LR and MRI-ESM2-0 models, all show high percentage values, and they are mainly due to larger maximum AMOC strength changes at 30°N ($\Delta\Psi$) (refer to Tab. 1), which further lead to larger temperature changes that caused by AMOC changes (ΔT_Ψ). For comparison, MPI-ESM1-2-LR and GISS-E2-1-G model, which both have very subtle changes in AMOC strength in *midHolocene*, reveal the AMOC changes contribute a minimal amount of the surface temperature changes (Fig. 5). After analysing all the models, we conclude that the AMOC does not play a globally important role in explaining the temperature changes. For most of the PMIP4 models (except for IPSL-CM6A-LR and MRI-ESM2-0 models), generally less than 30% of the temperature changes can be explained by the AMOC changes. Only some small regions show values close to 30%, while for other regions, there are minimal impacts of the AMOC on surface air temperature changes. This conclusion also applies to sea surface temperature and holds for the *lig127k* as well (not shown).

The percentage of precipitation changes that can be explained by AMOC changes has also been analysed, which can help us to explore whether or not the AMOC changes could be a mechanism for the precipitation changes discussed in proxy reconstructions. Since the plots which show the precipitation change that can be explained by AMOC change in individual models are not very clear to draw a distinct conclusion, we present an ensemble mean plot of the percentage of precipitation change that can be explained by AMOC change (Fig. 6). Then this ensemble mean plot (ΔP_Ψ / ΔP) is overlaid onto the

https://doi.org/10.5194/cp-2022-63
Preprint. Discussion started: 22 August 2022

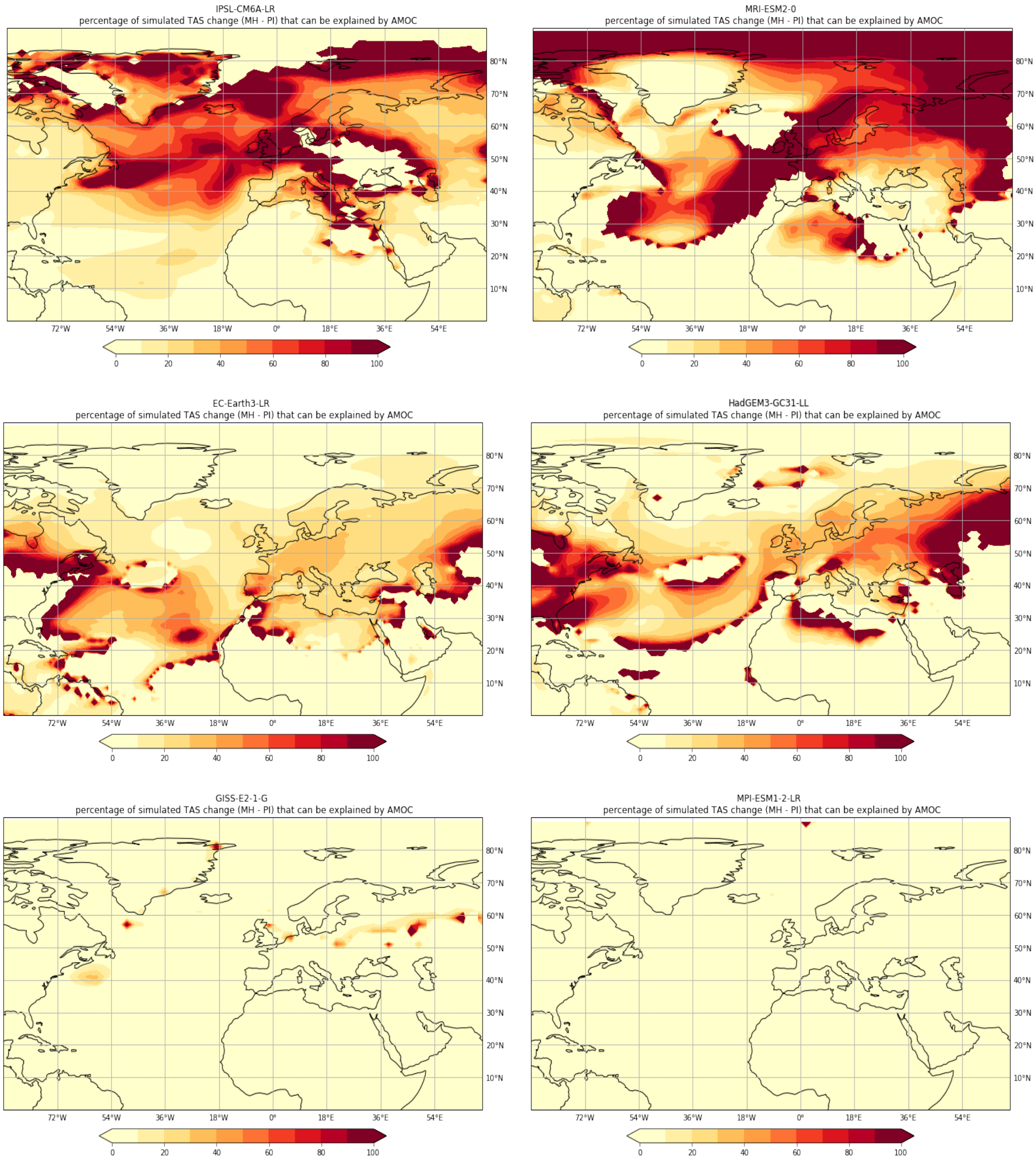

Figure 5. The percentage of *midHolocene* simulated surface temperature changes that could be explained by AMOC changes for six different models. The top 4 panels show the models with a ≥5% change in the maximum AMOC strength at 30°N, while the bottom two panels give examples of the low contribution.

https://doi.org/10.5194/cp-2022-63
Preprint. Discussion started: 22 August 2022

ensemble mean plot of the precipitation changes caused by AMOC changes (ΔP_{Ψ}), which is shown in Fig. 6. Similar plot has been made for the *lig127k* which is shown on the right panel.

The rainfall patterns associated with AMOC variations in the 2 interglacials are very similar (Fig. 6). The majority of regions across the global do not show any AMOC contributions to the precipitation changes. Only small Equatorial Pacific sections demonstrate at least 50% of the precipitation changes can be explained by the AMOC changes. Whether there is any physical reason for a strong AMOC influence to occur particularly in the Equatorial Pacific region still remain unclear. It further confirms our conclusion that, in practice, few precipitation changes can be explained by the AMOC changes. To summarise, the AMOC does not play a big role in explaining precipitation changes globally, and precipitation changes should not be used as an AMOC proxy according to our analysis.

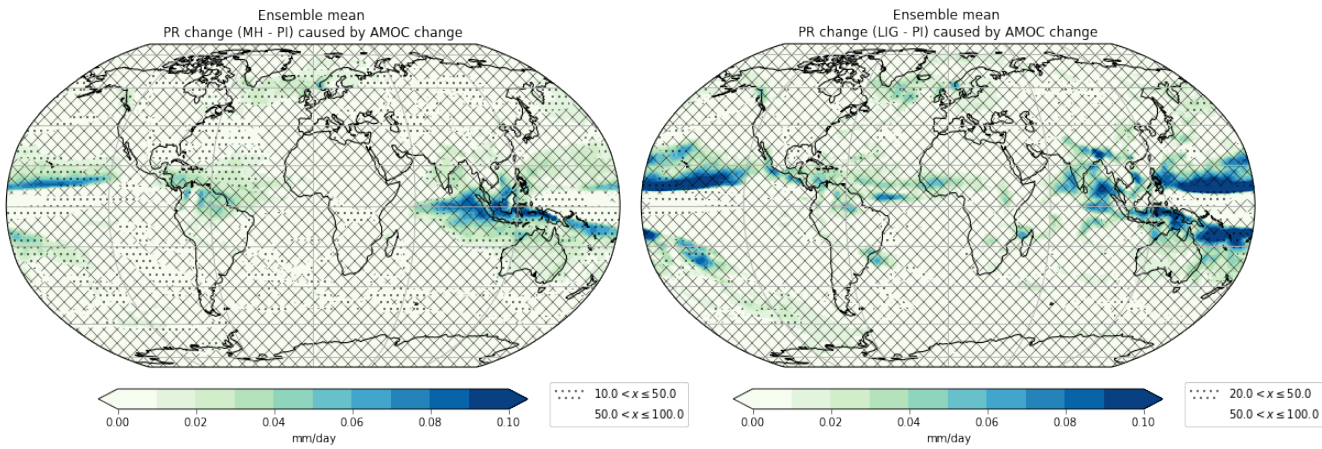

Figure 6. Ensemble mean plot of the precipitation changes caused by AMOC changes (ΔP_{Ψ}) at the *midHolocene* (left) and *lig127k* (right). Overlaid markers provide, the percentage of those changes that can be explained by AMOC changes ($100 \times \frac{\Delta P_{\Psi}}{\Delta P}$): no shading indicates that AMOC contributes half or more of the changes seen in the experiment, whilst the dotted symbol indicates a small contribution. Areas where there this no AMOC contribution are covered by crosshatching.

5 Discussion

Past changes in overall AMOC strength, especially its depth-integral, are difficult to reconstruct. One proxy technique is to use sedimentary Pa/Th (e.g. Yu et al., 1996; Bradtmiller et al., 2014), although modern geochemical observations highlight the contribution of other factors controlling the Pa and Th distribution (Hayes et al., 2013). Low resolution Pa/Th reconstructions available for the Holocene period indicates similar AMOC strength for the *midHolocene* and *piControl*, with the possibility of a slight weakening with time (McManus et al., 2004; Gherardi et al., 2009; Ng et al., 2018). This is supported by recent, high-resolution Holocene Pa/Th records from the North Atlantic (Hoffmann et al., 2018; Lippold et al., 2019), although these are single-site studies both from the subtropical Northwest Atlantic so it is unclear whether they represent the full AMOC.

https://doi.org/10.5194/cp-2022-63
Preprint. Discussion started: 22 August 2022

There are less reconstructed AMOC records for the last interglacial, although the sedimentary Pa/Th ratio (Guihou et al., 2010) suggests a similar AMOC strength compared to the *midHolocene* and *piControl*.

Reconstruction of changes in the density profile of the Florida Straits show little changes in the strength of the upper limb of the AMOC over the past 8000 years (Lynch-Stieglitz et al., 2009). Just under half the Florida Strait flow is associated with the AMOC, and the remainder is due to the wind-driven surface gyre circulation, such that the reported slight increase (4 Sv increase on a flow of 28-32 Sv) over the past 8000 years can likely be explained by changes in atmospheric circulation (Lynch-Stieglitz et al., 2009). To our knowledge, an equivalent reconstruction does not exist for the last interglacial.

In summary, no palaeo-reconstructions demonstrate substantive changes in the depth-integrated AMOC strength between either of the two interglacial states and the *piControl*. This, therefore, does not disagree with the PMIP4 ensemble demonstrating no consistent response in overall AMOC strength to the changes in orbital forcing (Sect. 3.2). However, uncertainties in the proxy data would need to be reduced significantly, and a greater number of proxy records obtained throughout the basin, to confidently assert that the PMIP4 ensemble is simulating the correct response (e.g. Burke et al., 2011). Many previous studies have instead focused on examining individual components of the AMOC or inferred changes in deep water mass geometry (e.g Kissel et al., 2013; Renssen et al., 2005). Further research into the various flow components of AMOC and their respective coupling to the climate system is required, before one could conclude that there were no significant interglacial changes in AMOC. It is also worth noting that all the simulations and analysis here is looking at equilibrated timeslice simulations, rather than transient simulations (Bader et al., 2020; Braconnot et al., 2019, e.g). Our conclusion of a minimal role for overall AMOC strength changes does not, therefore, apply to abrupt events where an AMOC response has long been identified (LeGrande and Schmidt, 2008).

6 Conclusions

The changes in mean AMOC strength in the *midHolocene* and *lig127k* have been investigated in this study using the PMIP4 models that performed the *midHolocene* and *lig127k* experiments, and they have been compared to the AMOC strength in the *piControl* experiment, respectively. Meanwhile, comparisons between the mean state of AMOC in the *midHolocene* and the *lig127k* have been made based on the ensemble mean. We further looked at the coherency across the two past interglacials for the forced response in AMOC, as well as the strength of the signal. A series of tests have been devised and four criteria identified to confirm an orbitally-forced response.

In all, the overall AMOC strength between either *lig127k* or *midHolocene* and *piControl* has not markedly changed in individual or model-averaged simulations (Fig. 1, Fig. 2). The two models that show the largest changes in the *lig127k* experiment change in the opposite direction. Many of the models show changes of amplitudes that could be explained by internal variability, rather an forced response (Williams et al., 2020). It therefore seems the changes in orbital forcing in both the *lig127k* and *midHolocene* experiment have very limited impact on the overall AMOC strength. This finding is not inconsistent with available proxy reconstructions. Obvious differences in the AMOC strength between individual models reveal that the climate

https://doi.org/10.5194/cp-2022-63
Preprint. Discussion started: 22 August 2022

Climate of the Past
Discussions
Open Access
EGU

Table A1. Digital Object Identifier (doi) for each simulation from CMIP6. The web address can be created manually by adding https://dx.doi.org/10.22033/ESGF/ in front of each doi. N/A in the Table indicates either that the simulation has not been performed, or that streamfunction data has not been uploaded to the Earth System Grid Federation.

Model	**Reference**	***midHolocene***	***lig127k***	***piControl***
CESM2	Otto-Bliesner et al. (2020)	CMIP6.7674	CMIP6.7673	CMIP6.7773
EC-Earth3-LR	Zhang et al. (2021)	CMIP6.4847	CMIP6.4798	CMIP6.4801
FGOALS-f3-L	Zheng et al. (2020)	CMIP6.12014	CMIP6.12013	CMIP6.3447
FGOALS-g3	Zheng et al. (2020)	CMIP6.3409	CMIP6.3407	CMIP6.3448
GISS-E2-1-G	Kelley et al. (2020)	CMIP6.7225	CMIP6.7223	CMIP6.7380
HadGEM3-GC31-LL	Williams et al. (2020)	CMIP6.12129	CMIP6.12128	CMIP6.6294
IPSL-CM6A-LR	Lurton et al. (2020)	CMIP6.5229	CMIP6.5228	CMIP6.5251
NorESM2-LM	Seland et al. (2020)	CMIP6.8079	CMIP6.8078	CMIP6.8217
INM-CM4-8	Volodin et al. (2018)	CMIP6.5077	CMIP6.5076	N/A
MPI-ESM1-2-LR	Scussolini et al. (2019)	CMIP6.6644	N/A	CMIP6.6675
MRI-ESM2-0	Yukimoto et al. (2019)	CMIP6.6860	N/A	CMIP6.6900
ACCESS-ESM1-5	Yeung et al. (2021)	N/A	CMIP6.13703	CMIP6.4312

models are still struggling to accurately simulate the present-day strength of the AMOC, as well as to capture the depth profile of the AMOC.

After investigating the changes in AMOC during the interglacials, we explored the AMOC roles in the surface climate. The spatial patterns arising from internal variability in the AMOC remains largely unchanged between the *midHolocene*, *lig127k* and *piControl*, although there are variations amongst the models in those patterns (Fig. 4). We demonstrate that the AMOC does not play a globally important role in explaining interglacial temperature changes in the majority of the PMIP4 models, with its effects only seen in the Nordic Seas and the south of Greenland in the mid-latitude North Atlantic (Fig. 5). Similarly, AMOC contributions to precipitation changes during the mid-Holocene and last interglacial occur in very few regions across the globe (Fig. 6), with the sole expection being the Northern Equatorial Pacific Ocean. Therefore, we strongly advise against interpreting hydrology-related proxy reconstructions as providing information about the AMOC. Combined with the inconsistent simulated forced response of AMOC during the PMIP4 timeslice simulations, the fingerprint analysis suggests that the overall AMOC strength changes should only be invoked to explain climate changes during abrupt events in interglacials.

Appendix A: ESGF Digital Object Identifier (doi)

https://doi.org/10.5194/cp-2022-63
Preprint. Discussion started: 22 August 2022

Code and data availability. Monthly output from each simulation can downloaded from the dois listed in Table A1. The code used for plotting the figures in this manuscript and all the processed output fields are available at the Github repository: https://github.com/pmip4/AMOC-during-the-interglacials-in-PMIP4-simulations-.

330 *Author contributions.* ZJ performed the bulk of analysis and writing. CB and DT conceived of the project and supervised ZJ during the research. S.S. contributed to the text related to the last interglacial. CB modified and deployed the Climate Variabiltiy Diagnostics Package, as well as editing the text.

Competing interests. The authors declare that they have no conflict of interest.

Acknowledgements. We would like to thank all the modelling groups who performed the PMIP experiments and generously made the
335 simulations output freely available. We also thank Zarina Hewett as an internal reviewer for her comments on this manuscript, and Adam Phillips and Jon Fasullo for developing the CVDP.

.

https://doi.org/10.5194/cp-2022-63
Preprint. Discussion started: 22 August 2022

Climate of the Past
Discussions

References

Bader, J., Jungclaus, J., Krivova, N., Lorenz, S., Maycock, A., Raddatz, T., Schmidt, H., Toohey, M., Wu, C. J., and Claussen, M.: Global temperature modes shed light on the Holocene temperature conundrum, Nature Communications, 11, https://doi.org/10.1038/s41467-020-18478-6, 2020.

Berger, A. and Loutre, M. F.: Insolation values for the climate of the last 10 million years, Quaternary Science Reviews, 10, 297–317, https://doi.org/10.1016/0277-3791(91)90033-Q, 1991.

Bonnet, R., Boucher, O., Deshayes, J., Gastineau, G., Hourdin, F., Mignot, J., Servonnat, J., and Swingedouw, D.: Presentation and evaluation of the IPSL-CM6A-LR Ensemble of extended historical simulations, Journal of Advances in Modeling Earth Systems, 13, e2021MS002 565, 2021.

Borchert, L. F., Müller, W. A., and Baehr, J.: Atlantic ocean heat transport influences interannual-to-decadal surface temperature predictability in the North Atlantic region, Journal of Climate, 31, 6763–6782, 2018.

Braconnot, P., Zhu, D., Marti, O., and Servonnat, J.: Strengths and challenges for transient Mid- to Late Holocene simulations with dynamical vegetation, Climate of the Past, 15, 997–1024, https://doi.org/10.5194/cp-15-997-2019, 2019.

Bradtmiller, L. I., McManus, J. F., and Robinson, L. F.: 231Pa/230Th evidence for a weakened but persistent Atlantic meridional overturning circulation during Heinrich Stadial 1, Nature Communications, 5, 1–8, 2014.

Brierley, C. M., Zhao, A., Harrison, S. P., Braconnot, P., Williams, C. J., Thornalley, D. J., Shi, X., Peterschmitt, J. Y., Ohgaito, R., Kaufman, D. S., Kageyama, M., Hargreaves, J. C., Erb, M. P., Emile-Geay, J., D'Agostino, R., Chandan, D., Carré, M., Bartlein, P. J., Zheng, W., Zhang, Z., Zhang, Q., Yang, H., Volodin, E. M., Tomas, R. A., Routson, C., Richard Peltier, W., Otto-Bliesner, B., Morozova, P. A., McKay, N. P., Lohmann, G., Legrande, A. N., Guo, C., Cao, J., Brady, E., Annan, J. D., and Abe-Ouchi, A.: Large-scale features and evaluation of the PMIP4-CMIP6 midHolocene simulations, Climate of the Past, 16, 1847–1872, https://doi.org/10.5194/cp-16-1847-2020, 2020.

Buckley, M. W. and Marshall, J.: Observations, inferences, and mechanisms of the Atlantic Meridional Overturning Circulation: A review, Reviews of Geophysics, 54, 5–63, 2016.

Burke, A., Marchal, O., Bradtmiller, L. I., McManus, J. F., and François, R.: Application of an inverse method to interpret 231Pa/230Th observations from marine sediments, Paleoceanography, 26, 2011.

Capron, E., Govin, A., Feng, R., Otto-Bliesner, B. L., and Wolff, E. W.: Critical evaluation of climate syntheses to benchmark CMIP6/PMIP4 127 ka Last Interglacial simulations in the high-latitude regions, Quaternary Science Reviews, 168, 137–150, https://doi.org/10.1016/j.quascirev.2017.04.019, 2017.

Chen, X. and Tung, K. K.: Varying planetary heat sink led to global-warming slowdown and acceleration, Science, 345, 897–903, https://doi.org/10.1126/science.1254937, 2014.

Chen, X. and Tung, K.-K.: Global surface warming enhanced by weak Atlantic overturning circulation, Nature, 559, 387–391, 2018.

Danabasoglu, G., Yeager, S. G., Kwon, Y. O., Tribbia, J. J., Phillips, A. S., and Hurrell, J. W.: Variability of the atlantic meridional overturning circulation in CCSM4, Journal of Climate, 25, 5153–5172, https://doi.org/10.1175/JCLI-D-11-00463.1, 2012.

Eyring, V., Bony, S., Meehl, G. A., Senior, C. A., Stevens, B., Stouffer, R. J., and Taylor, K. E.: Overview of the Coupled Model Intercomparison Project Phase 6 (CMIP6) experimental design and organization, Geoscientific Model Development, 9, 1937–1958, https://doi.org/10.5194/gmd-9-1937-2016, 2016.

Fischer, N.: Holocene and Eemian climate variability, Ph.D. thesis, University of Hamburg Hamburg, 2011.

https://doi.org/10.5194/cp-2022-63
Preprint. Discussion started: 22 August 2022

Climate of the Past Discussions

Gherardi, J.-M., Labeyrie, L., Nave, S., François, R., McManus, J. F., and Cortijo, E.: Glacial-interglacial circulation changes inferred from 231Pa/230Th sedimentary record in the North Atlantic region, Paleoceanography, 24, 2009.

Gruber, N., Keeling, C. D., and Bates, N. R.: Interannual variability in the North Atlantic Ocean carbon sink, Science, 298, 2374–2378, 2002.

Guihou, A., Pichat, S., Nave, S., Govin, A., Labeyrie, L., Michel, E., and Waelbroeck, C.: Late slowdown of the Atlantic meridional overturning circulation during the last glacial inception: new constraints from sedimentary (231Pa/230Th), Earth and Planetary Science Letters, 289, 520–529, 2010.

Găinuşă-Bogdan, A., Swingedouw, D., Yiou, P., Cattiaux, J., Codron, F., and Michel, S.: AMOC and summer sea ice as key drivers of the spread in mid-holocene winter temperature patterns over Europe in PMIP3 models, Global and Planetary Change, 184, https://doi.org/10.1016/j.gloplacha.2019.103055, 2020.

Hayes, C. T., Anderson, R. F., Fleisher, M. Q., Serno, S., Winckler, G., and Gersonde, R.: Quantifying lithogenic inputs to the North Pacific Ocean using the long-lived thorium isotopes, Earth and Planetary Science Letters, 383, 16–25, 2013.

Hoffmann, S. S., McManus, J. F., and Swank, E.: Evidence for stable Holocene basin-scale overturning circulation despite variable currents along the deep western boundary of the North Atlantic Ocean, Geophysical Research Letters, 45, 13–427, 2018.

Jackson, L. and Wood, R.: Fingerprints for early detection of changes in the AMOC, Journal of Climate, 33, 7027–7044, 2020.

Joussaume, S. and Braconnot, P.: Sensitivity of paleoclimate simulation results to season definitions, Journal of Geophysical Research Atmospheres, 102, 1943–1956, https://doi.org/10.1029/96jd01989, 1997.

Jungclaus, J. H., Lohmann, K., and Zanchettin, D.: Enhanced 20th-century heat transfer to the Arctic simulated in the context of climate variations over the last millennium, Climate of the Past, 10, 2201–2213, 2014.

Kageyama, M., Braconnot, P., Harrison, S. P., Haywood, A. M., Jungclaus, J. H., Otto-Bliesner, B. L., Abe-Ouchi, A., Albani, S., Bartlein, P. J., Brierley, C., Crucifix, M., Dolan, A., Fernandez-Donado, L. L., Fischer, H., Hopcroft, P. O., Ivanovic, R. F., Lambert, F., Lunt, D. J., Mahowald, N. M., Richard Peltier, W., Phipps, S. J., Roche, D. M., Schmidt, G. A., Tarasov, L., Valdes, P. J., Zhang, Q., and Zhou, T.: The PMIP4 contribution to CMIP6 - Part 1: Overview and over-arching analysis plan, Geoscientific Model Development, 11, 1033–1057, https://doi.org/10.5194/gmd-11-1033-2018, 2018.

Kelley, M., Schmidt, G. A., Nazarenko, L. S., Bauer, S. E., Ruedy, R., Russell, G. L., Ackerman, A. S., Aleinov, I., Bauer, M., Bleck, R., et al.: GISS-E2. 1: Configurations and climatology, Journal of Advances in Modeling Earth Systems, 12, e2019MS002 025, 2020.

Kissel, C., Van Toer, A., Laj, C., Cortijo, E., and Michel, E.: Variations in the strength of the North Atlantic bottom water during Holocene, Earth and Planetary Science Letters, 369-370, 248–259, https://doi.org/10.1016/j.epsl.2013.03.042, 2013.

Kuhlbrodt, T., Griesel, A., Montoya, M., Levermann, A., Hofmann, M., and Rahmstorf, S.: On the driving processes of the Atlantic meridional overturning circulation, https://doi.org/10.1029/2004RG000166, 2007.

Latif, M., Sun, J., Visbeck, M., and Hadi Bordbar, M.: Natural variability has dominated Atlantic Meridional Overturning Circulation since 1900, Nature Climate Change, pp. 1–6, 2022.

LeGrande, A. N. and Schmidt, G. A.: Ensemble, water isotope–enabled, coupled general circulation modeling insights into the 8.2 ka event, Paleoceanography, 23, 2008.

Lippold, J., Pöppelmeier, F., Süfke, F., Gutjahr, M., Goepfert, T. J., Blaser, P., Friedrich, O., Link, J. M., Wacker, L., Rheinberger, S., et al.: Constraining the variability of the Atlantic meridional overturning circulation during the Holocene, Geophysical Research Letters, 46, 11 338–11 346, 2019.

Lozier, M. S., Li, F., Bacon, S., Bahr, F., Bower, A. S., Cunningham, S. A., De Jong, M. F., De Steur, L., DeYoung, B., Fischer, J., Gary, S. F., Greenan, B. J., Holliday, N. P., Houk, A., Houpert, L., Inall, M. E., Johns, W. E., Johnson, H. L., Johnson, C., Karstensen, J., Koman, G., Le Bras, I. A., Lin, X., Mackay, N., Marshall, D. P., Mercier, H., Oltmanns, M., Pickart, R. S., Ramsey, A. L., Rayner, D., Straneo, F., Thierry, V., Torres, D. J., Williams, R. G., Wilson, C., Yang, J., Yashayaev, I., and Zhao, J.: A sea change in our view of overturning in the subpolar North Atlantic, Science, 363, 516–521, https://doi.org/10.1126/science.aau6592, 2019.

Lurton, T., Balkanski, Y., Bastrikov, V., Bekki, S., Bopp, L., Braconnot, P., Brockmann, P., Cadule, P., Contoux, C., Cozic, A., et al.: Implementation of the CMIP6 Forcing Data in the IPSL-CM6A-LR Model, Journal of Advances in Modeling Earth Systems, 12, e2019MS001 940, 2020.

Lynch-Stieglitz, J., Curry, W. B., and Lund, D. C.: Florida Straits density structure and transport over the last 8000 years, Paleoceanography, 24, 2009.

McKay, N. P., Kaufman, D. S., Routson, C. C., Erb, M. P., and Zander, P. D.: The onset and rate of Holocene Neoglacial cooling in the Arctic, Geophysical Research Letters, 45, 12–487, 2018.

McManus, J. F., Francois, R., Gherardl, J. M., Kelgwin, L., and Drown-Leger, S.: Collapse and rapid resumption of Atlantic meridional circulation linked to deglacial climate changes, Nature, 428, 834–837, https://doi.org/10.1038/nature02494, 2004.

Ng, H. C., Robinson, L. F., McManus, J. F., Mohamed, K. J., Jacobel, A. W., Ivanovic, R. F., Gregoire, L. J., and Chen, T.: Coherent deglacial changes in western Atlantic Ocean circulation, Nature communications, 9, 1–10, 2018.

Otto-Bliesner, B. L., Braconnot, P., Harrison, S. P., Lunt, D. J., Abe-Ouchi, A., Albani, S., Bartlein, P. J., Capron, E., Carlson, A. E., Dutton, A., Fischer, H., Goelzer, H., Govin, A., Haywood, A., Joos, F., Legrande, A. N., Lipscomb, W. H., Lohmann, G., Mahowald, N., Nehrbass-Ahles, C., Pausata, F. S., Peterschmitt, J. Y., Phipps, S. J., Renssen, H., and Zhang, Q.: The PMIP4 contribution to CMIP6 - Part 2: Two interglacials, scientific objective and experimental design for Holocene and Last Interglacial simulations, Geoscientific Model Development, 10, 3979–4003, https://doi.org/10.5194/gmd-10-3979-2017, 2017.

Otto-Bliesner, B. L., Brady, E. C., Tomas, R. A., Albani, S., Bartlein, P. J., Mahowald, N. M., Shafer, S. L., Kluzek, E., Lawrence, P. J., Leguy, G., et al.: A comparison of the CMIP6 midHolocene and lig127k simulations in CESM2, Paleoceanography and Paleoclimatology, 35, e2020PA003 957, 2020.

Petit, T., Lozier, M. S., Josey, S. A., and Cunningham, S. A.: Role of air–sea fluxes and ocean surface density in the production of deep waters in the eastern subpolar gyre of the North Atlantic, Ocean science, 17, 1353–1365, 2021.

Phillips, A. S., Deser, C., and Fasullo, J.: Evaluating modes of variability in climate models, Eos, 95, 453–455, https://doi.org/10.1002/2014EO490002, 2014.

Rahmstorf, S.: Thermohaline ocean circulation, in: Encyclopedia of Quaternary Sciences, edited by Elias, S. A., pp. 1–10, Elsevier, Amsterdam, 2006.

Rayner, D., Hirschi, J. J., Kanzow, T., Johns, W. E., Wright, P. G., Frajka-Williams, E., Bryden, H. L., Meinen, C. S., Baringer, M. O., Marotzke, J., Beal, L. M., and Cunningham, S. A.: Monitoring the Atlantic meridional overturning circulation, Deep-Sea Research Part II: Topical Studies in Oceanography, 58, 1744–1753, https://doi.org/10.1016/j.dsr2.2010.10.056, 2011.

Renssen, H., Goosse, H., and Fichefet, T.: Contrasting trends in North Atlantic deep-water formation in the Labrador Sea and Nordic Seas during the Holocene, Geophysical Research Letters, 32, 1–4, https://doi.org/10.1029/2005GL022462, 2005.

Scussolini, P., Bakker, P., Guo, C., Stepanek, C., Zhang, Q., Braconnot, P., Cao, J., Guarino, M.-V., Coumou, D., Prange, M., et al.: Agreement between reconstructed and modeled boreal precipitation of the Last Interglacial, Science advances, 5, eaax7047, 2019.

Seland, Ø., Bentsen, M., Olivié, D., Toniazzo, T., Gjermundsen, A., Graff, L. S., Debernard, J. B., Gupta, A. K., He, Y.-C., Kirkevåg, A., et al.: Overview of the Norwegian Earth System Model (NorESM2) and key climate response of CMIP6 DECK, historical, and scenario simulations, Geoscientific Model Development, 13, 6165–6200, 2020.

https://doi.org/10.5194/cp-2022-63
Preprint. Discussion started: 22 August 2022

Climate of the Past
Discussions

Shi, X. and Lohmann, G.: Simulated response of the mid-Holocene Atlantic meridional overturning circulation in ECHAM6-FESOM/MPIOM, Journal of Geophysical Research: Oceans, 121, 6444–6469, 2016.

Srokosz, M., Baringer, M., Bryden, H., Cunningham, S., Delworth, T., Lozier, S., Marotzke, J., and Sutton, R.: Past, present, and future changes in the atlantic meridional overturning circulation, Bulletin of the American Meteorological Society, 93, 1663–1676, https://doi.org/10.1175/BAMS-D-11-00151.1, 2012.

Steinman, B. A., Mann, M. E., and Miller, S. K.: Atlantic and Pacific multidecadal oscillations and Northern Hemisphere temperatures, Science, 347, 988–991, https://doi.org/10.1126/science.1257856, 2015.

Tung, K. K. and Zhou, J.: Using data to attribute episodes of warming and cooling in instrumental records, Proceedings of the National Academy of Sciences of the United States of America, 110, 2058–2063, https://doi.org/10.1073/pnas.1212471110, 2013.

Volodin, E. M., Mortikov, E. V., Kostrykin, S. V., Galin, V. Y., Lykossov, V. N., Gritsun, A. S., Diansky, N. A., Gusev, A. V., Iakovlev, N. G., Shestakova, A. A., et al.: Simulation of the modern climate using the INM-CM48 climate model, Russian Journal of Numerical Analysis and Mathematical Modelling, 33, 367–374, 2018.

Williams, C. J. R., Guarino, M.-V., Capron, E., Malmierca-Vallet, I., Singarayer, J. S., Sime, L. C., Lunt, D. J., and Valdes, P. J.: CMIP6/PMIP4 simulations of the mid-Holocene and Last Interglacial using HadGEM3: comparison to the pre-industrial era, previous model versions and proxy data, Climate of the Past, 16, 1429–1450, 2020.

Yeung, N. K.-H., Menviel, L., Meissner, K. J., Taschetto, A. S., Ziehn, T., and Chamberlain, M.: Land–sea temperature contrasts at the Last Interglacial and their impact on the hydrological cycle, Climate of the Past, 17, 869–885, 2021.

Yu, E.-F., Francois, R., and Bacon, M. P.: Similar rates of modern and last-glacial ocean thermohaline circulation inferred from radiochemical data, Nature, 379, 689–694, 1996.

Yukimoto, S., Kawai, H., Koshiro, T., Oshima, N., Yoshida, K., Urakawa, S., Tsujino, H., Deushi, M., Tanaka, T., Hosaka, M., et al.: The Meteorological Research Institute Earth System Model version 2.0, MRI-ESM2. 0: Description and basic evaluation of the physical component, Journal of the Meteorological Society of Japan. Ser. II, 2019.

Zhang, Q., Berntell, E., Axelsson, J., Chen, J., Han, Z., De Nooijer, W., Lu, Z., Li, Q., Zhang, Q., Wyser, K., et al.: Simulating the mid-Holocene, last interglacial and mid-Pliocene climate with EC-Earth3-LR, Geoscientific Model Development, 14, 1147–1169, 2021.

Zhao, A., Brierley, C. M., Jiang, Z., Eyles, R., Oyarzún, D., and Gomez-Dans, J.: Analysing the PMIP4-CMIP6 collection: a workflow and tool (pmip_p2fvar_analyzer v1), Geoscientific Model Development, 15, 2475–2488, 2022.

Zheng, W., Yu, Y., Luan, Y., Zhao, S., He, B., Dong, L., Song, M., Lin, P., and Liu, H.: CAS-FGOALS Datasets for the Two Interglacial Epochs of the Holocene and the Last Interglacial in PMIP4, Advances in Atmospheric Sciences, 37, 1034–1044, 2020.